Nanopatterning Utilizing Molecular Recognition
And Progress Towards the Synthesis of Molecular Wires

Kevin Barry

Research Advisor: Prof. Amar H. Flood

C500 Final Report
April 21, 2006

Introduction

The focus of the research that has been conducted for this report describes progress made (1) toward nano-patterned surfaces and (2) toward the synthesis of molecular wires and their future in the field of molecular electronics.

Nano-Patterning

Building upon a biologically dominated concept of self-assembly a young field of chemistry has emerged to study the generation of self-assembled monolayers (SAMs). Defined in 1983, a self-assembling monolayer is the process by which molecules spontaneously form ordered aggregates on a surface through noncovalent and covalent interactions of the individual units.[1,2] The interactions, mainly noncovalent, shape the resulting supramolecular structure in variable dimensions.[3] In these systems, reversibility, especially reversible non-covalent interactions, is important so that the pieces which the aggregate is composed of have the ability to adjust their positions relative to the other units to form a monolayer without defects.[1] Due to the specificity of interactions between units and between units and the surface, it is possible to conceive how the building blocks could be designed to have directed interactions and thus, be tailored to form a desired pattern on a surface.

Biological examples of self-assembly are some of the most pervasive and well known. The self-assembly of DNA double helices due to complementary hydrogen bonding interactions between the nucleobase pairings of guanine with cytosine, and adenine with thymine (Figure 1), has inspired the incorporation of these base pairs into molecules so as to utilize the pairing for the self assembly of supramolecular structures.

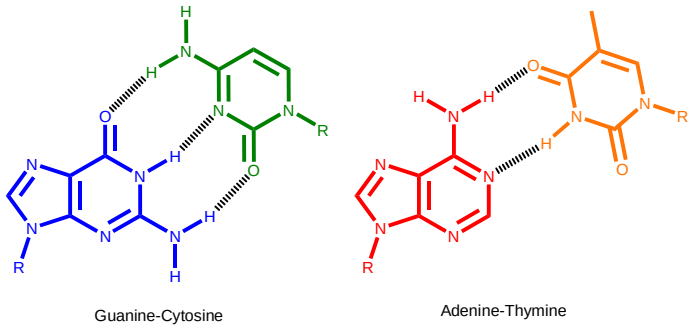

Figure 1: Watson-Crick nucleobase pairing motif

For example this base pairing motif has been used to to generate self-assembling dimers of dinucleoside precursors.[4,5] The nucleobases have several pairing modes which can be utilized for the generation of supramolecular structures such as the classical Watson-Crick, reverse Watson-Crick, Wobble,[4] and Hoogsteen[4,6] pairings.

In forming an organized SAM, the connection to the surface for film formation needs to be accounted for in the design of target molecules as much as for interactions between the molecules themselves. More over, SAM formation is driven ethalpically by the surface-to-headgroup bonding to overcome the entropic loss. The type of interaction with the surface depends on the surface being used. Since self-assembly is a desired trait in film formation, a headgroup with an affinity for the surface needs to be incorporated into the self-assembling molecule. Common surfaces on which SAMs are formed are gold,[7-9] silver,[9] copper,[10] and silicon oxide.[2] When using gold surfaces, a thiol-linkage (RSH) is commonly used due to the aurophilic nature of thiols,[7,8] but dialkyl sulfides (R-S-R') and dialkyldisulfides (R-S-S-R') are also utilized. A terpyridine ligand with a thiol linker can be used to add further functionality to a SAM on account of the open tridentate coordination sphere of the terpyridine ligand towards transition metal moieties such as those based on Fe or Ru.[7,8] With only one thiol functionality, the transition metal complex

would have one surface-binding mode, greatly reducing the possibility of surface binding defects.

The technological driver of micro-to-nano fabrication and the pervasive, ever present examples of natural self-assembly have inspired us to develop molecular systems to direct the formation of patterned surfaces with nanometer resolution. Our intention is to lay the foundation on which to build larger structures, hybridize with top-down engineering approaches and/or establish a platform on which to perform molecular scale activities.

The molecular design and synthesis of symmetric terpyridine ligands incorporating nucleobase functionalities directed along the ligands long axis for inclusion into larger supramolecular complexes have been proposed (Figure 2**)**.

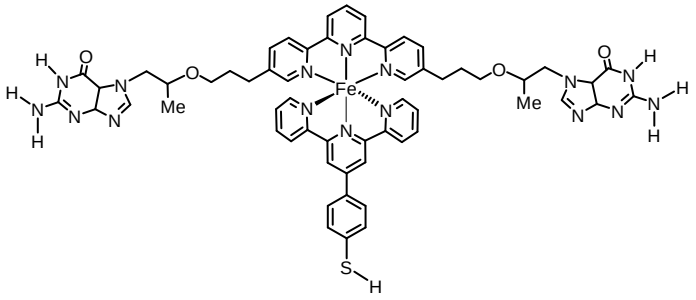

(a)

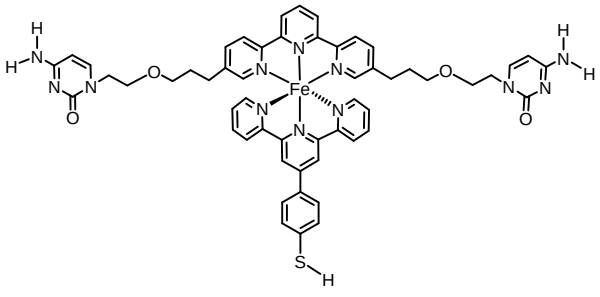

(b)

Figure 2: Supramolecular structure of terpyridine complexes containing (a) guanine functionalities and (b) cytosine functionalities.

Based on established synthetic methodologies, the following potential synthetic approaches (Scheme 1-3) for the synthesis of terpyridine ligands (Scheme 1), alkylated nucleobase precursor synthons (Scheme 2), and connection strategies between the nucleobases to the terpy ligands (Scheme 3) have been proposed. In Scheme 1, the precursor 2-acetyl-5-methylpyridine (**2**) used previously in the formation of **4**[11] (based on the general terpyridine synthesis[12] reported by Jameson), must be generated from 2-bromo-5-methylpyridine.[13] An important qualitative feature of the approach outlined in Scheme 1 is that it provides the ability to generate asymmetric terpyridine ligands in the future based on the preparation of β-(dimethylamino)vinyl 2-pyridyl ketone from 2-acetyl pyridine,[13] and then further reaction with a second 2-acetyl pyridine with an additional substituent (Scheme 4). Terpyridine ligand **4** will subsequently be functionalized to a di-hydroxypropyl terpyridine ligand (**7**).[11] Adding the hydroxyl functional groups provides functional sites where the alkylated nucleobases,[5] guanine and cytosine, can be connected covalently to the terpyridine core (Scheme 3).

Scheme 1: Synthesis of symmetric terpyridine ligands. (Dotted arrows reflect planned syntheses and dotted box yields are predicted from literature methods.)

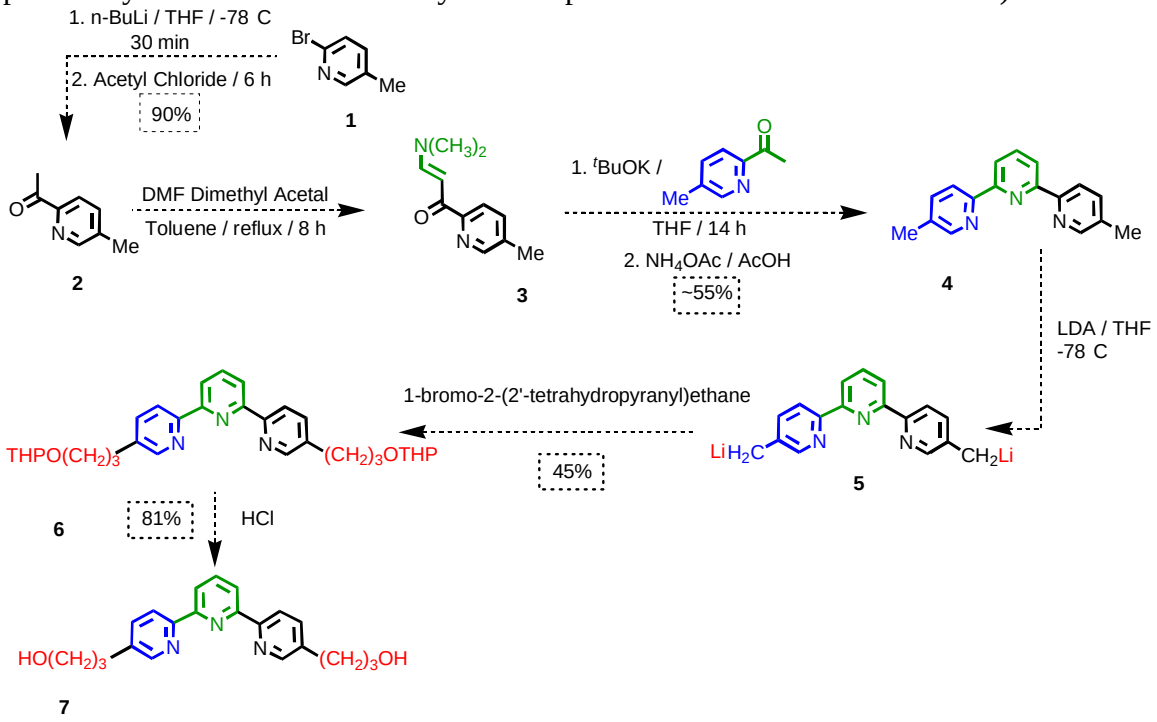

Scheme 2: Alkylation of nucleobases

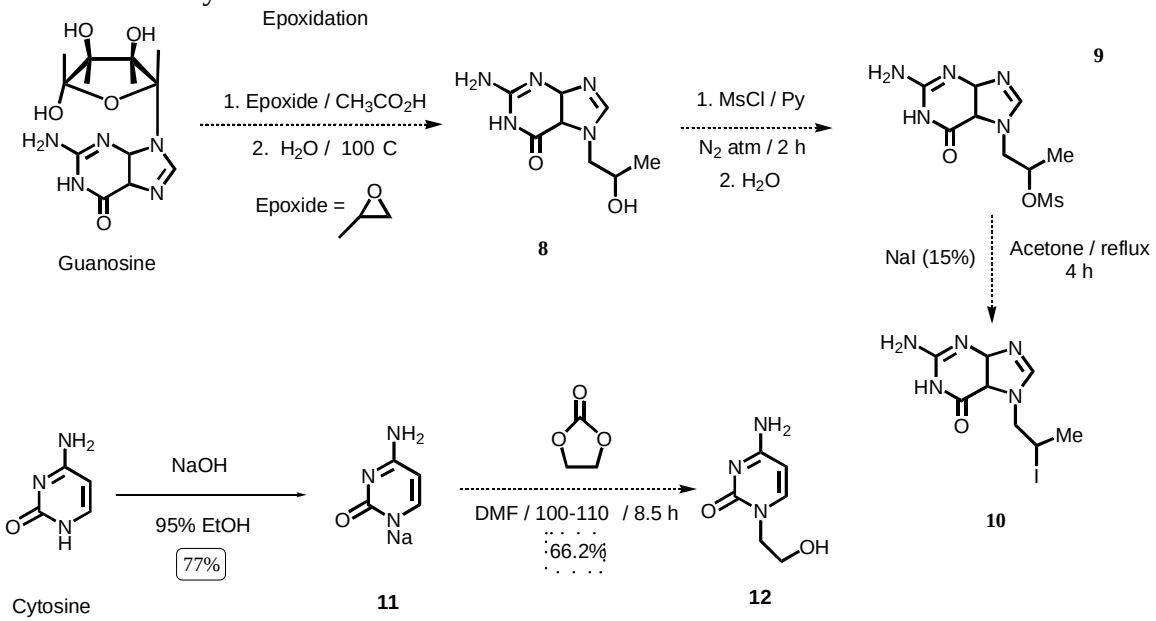

Scheme 3: Potential strategies for the connection of alkylated nucleobases (NB) to the terpyridine ligand core.

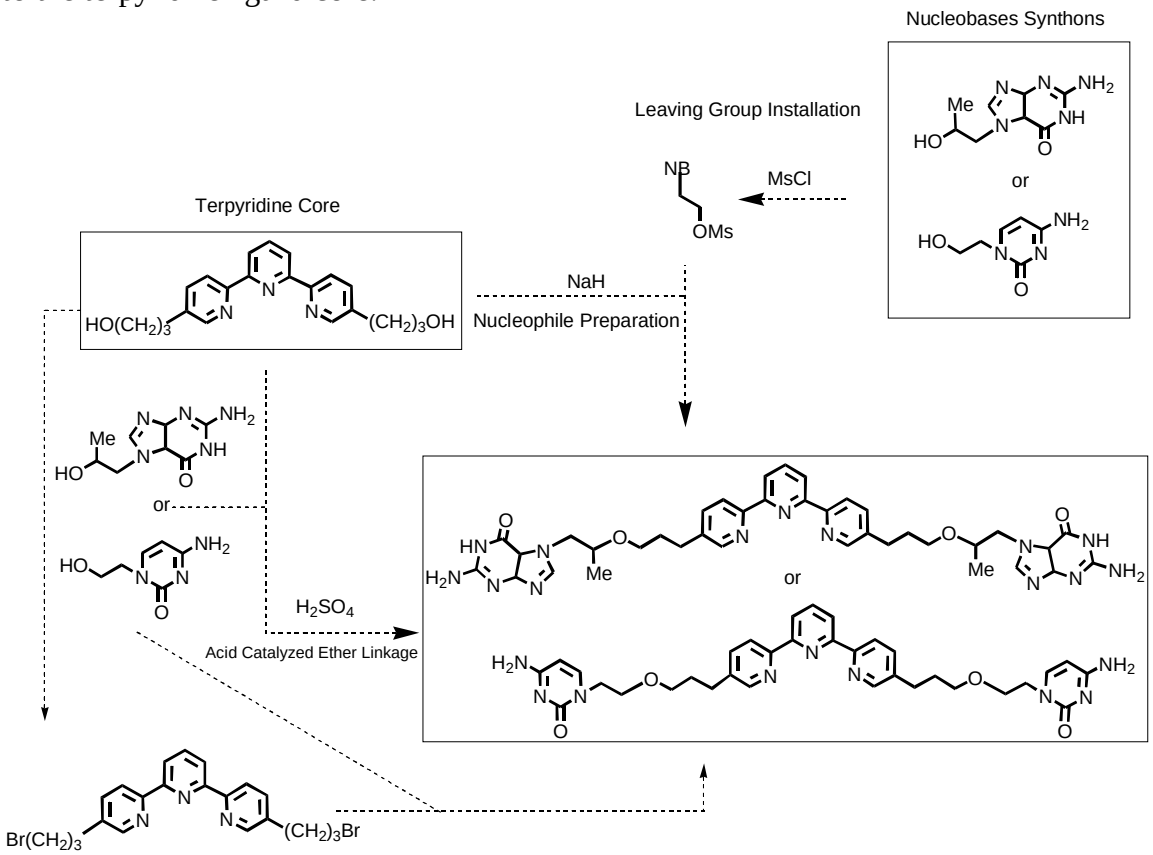

Scheme 4: Strategy for the synthesis of an asymmetric terpyridine

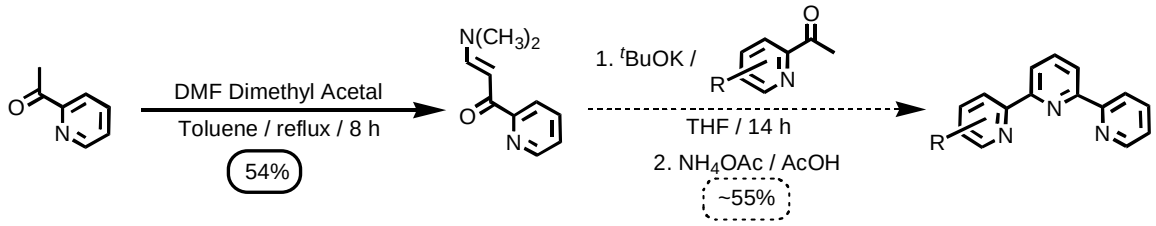

Molecular Wires

Current standard electronics are dominated by silicon based semiconductor technologies. As the desire and demand for faster and smaller electronic items such as computers has grown, the need to reduce the size of the silicon based structural features has also grown accordingly. Presently technology allowing for these small-scale features

has been able to keep up with demand. However, conventional silicon based electronics are reaching their physical limits.[14] When this limit will be finally be reached cannot be pinpointed on a calendar; yet when this time arrives, the demand for improved capability, capacity, size, and convenience will not reach its limit as well.

It is because of this demand that research into future nano-scale and molecular electronic systems must be conducted. There are several factors of concern that would cause silicon-based electronics at the molecular scale to be unfeasible. For example, the necessity for doping with boron or arsenic may cause erratic behavior.[15] Other concerns including the gate oxide thickness, high power consumption, and large production cost would be typical of scaling silicon electronics to the molecular scale.[15] Single molecules on the other hand have properties that, when ordered on a small surface area at high density, would be much more favorable to continued advancement of electronic technologies. Molecules have the ultimate advantage in size and control over physical properties at the atomic level[15] because they can be designed and tailored as needed within synthetic limitations which are themselves continuously expanding.

The idea behind molecular electronics as it is perceived today began in 1974 with the proposal of a molecular rectifier, a diode which causes electronic current to flow in only one direction, by Aviram and Ratner, an example of which is shown in Figure 3.[16] Their work demonstrated the feasibility of passing current through organic molecules in a cathode-acceptor-donor-anode motion, where the acceptor and donor are located within the molecule and separated by bridge, in the given example a triple methylene bridge, to increase rigidity as well as ensure the π levels of the acceptor and donor are non-interacting.[16]

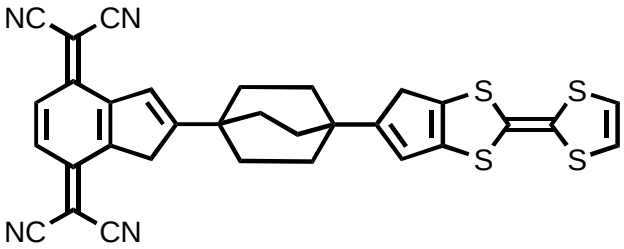

Figure 3: Molecular rectifier

The idea that molecular electronics is a viable path is further supported by the knowledge that electronic processes, both storage and transfer, in biological systems occur through molecular structures,[15,16] organic and inorganic. And so it has become a major goal to put molecules to work by utilizing their physical and chemical properties.[14] Molecules have been fashioned in such ways as to generate molecular gears stimulated by the addition or removal of an electron,[17] molecule cascades,[18] and molecular wires[19,20] among other things.

Molecular wires have the potential to be chemically very diverse, however, they generally fall into two divisions: complexes of highly conjugated organic bridges connecting two more metal centers (Figure 4a), and molecules with or without bridging ligands but containing metal-metal bonds.[21,22] Highly conjugated strictly organic frameworks (Figure 4b) can also work as molecular wires[22], however, the inclusion of metal centers reduces the distance of the ligands' HOMO π to LUMO π* gap thus making conduction of electricity through the molecule a lower energy process.

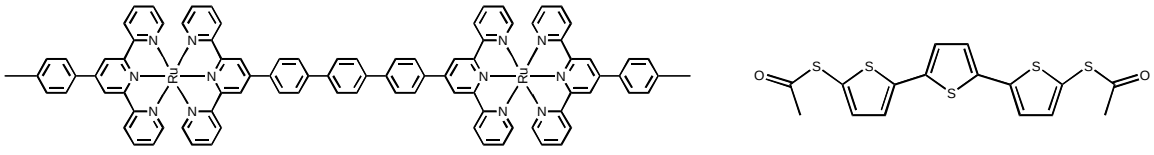

Figure 4: Examples of Molecular Wires, Inorganic and Organic

The progress toward molecular wires discussed herein is that of the generation of mixed valent di-ruthenium based molecules of the general form seen in Scheme 5. These molecules have the potential for future applications as the active device components of electronic circuitry or for inclusion as part of molecular-mechanical switches that form the foundation for random access memory circuits[15] found in all manner of devices from washing machines to digital cameras to vacuum cleaners. Synthesis of both mononuclear (Scheme 6) and dinuclear ruthenium complexes (Scheme 7) as well as challenges encountered in the synthesis and the resulting purity will all be discussed. The characterization of these compounds and a model bisthione compound (Scheme 8) will be presented.[1]

Scheme 5: Target Molecular Wires

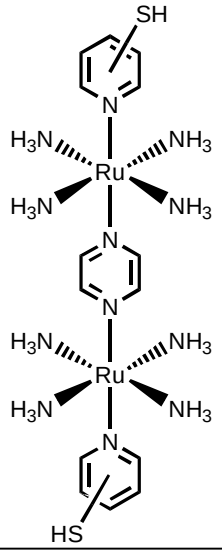

Scheme 6: Synthesis of mononuclear pentaamine ruthenium complexes

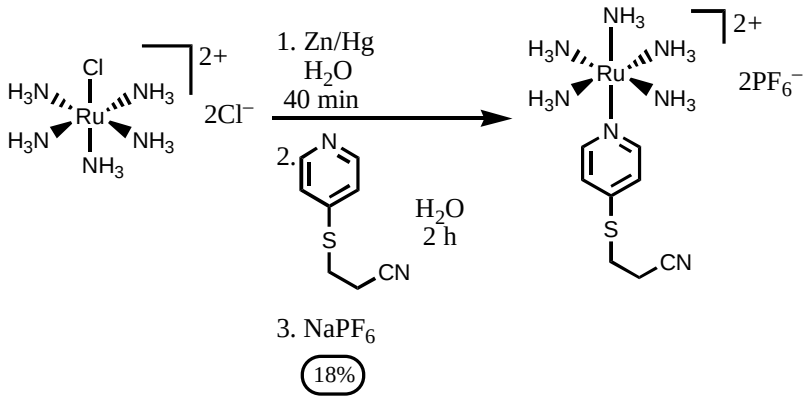

[1] P. Chand, 2005, Indiana University

Scheme 7: Synthesis of binuclear ruthenium molecular wires

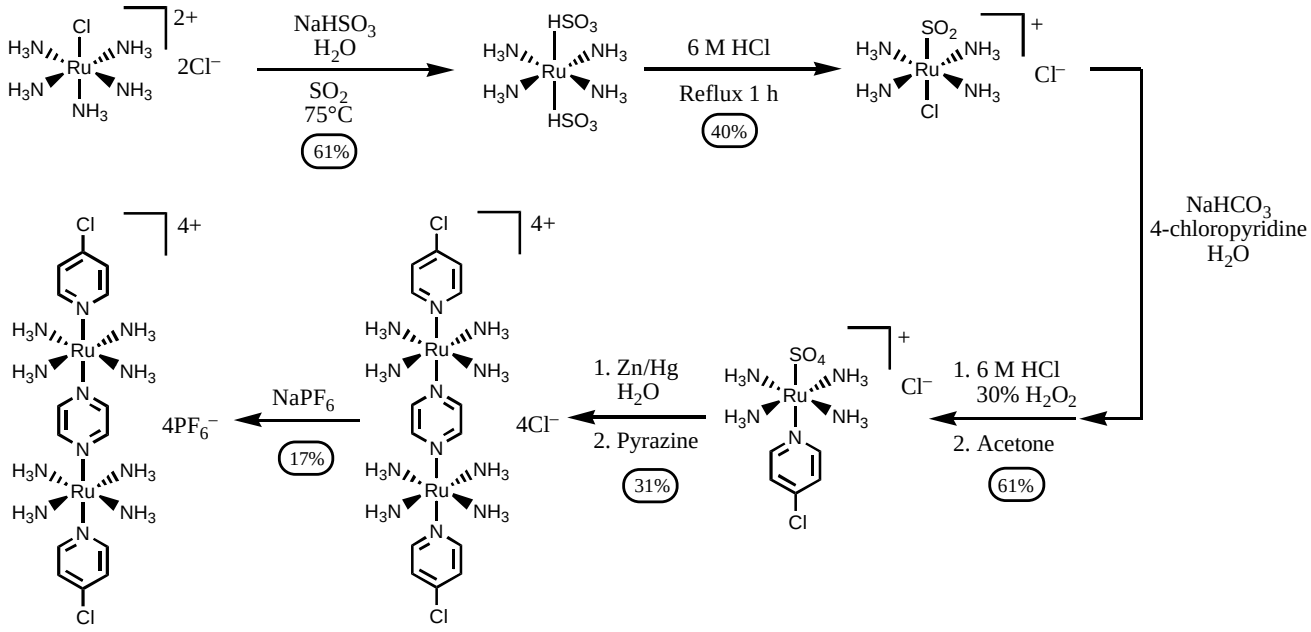

Scheme 8: [Ru(py)4(thione)2]•2PF_6

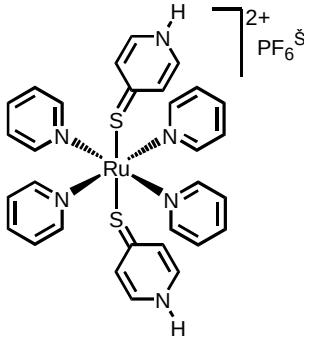

The bisthione, [Ru(py)4(thione)2]•2PF_6, was an unintended result on the path toward the synthesis of molecular wires. However, the bisthione ruthenium(II)tetrapyridine complex represents an interesting "null" control system on account of the fact that the sulfur is bound to the ruthenium center.

The 4-mercaptopyridine (not shown) is the preferred mode of binding through the nitrogen, yet tautomerism to the thione appears facile for a ruthenium center with a high

charge density. It is possible that the electrochemical studies performed on this compound could provide signatures of sulfur-coordinated ruthenium (III/II) centers and therefore a means to identify these coordination modes should they emerge during studies of nitrogen-bound mercapto compounds.

1 Experimental

1.1 General Procedures

All preparative reactions and purifications were carried out under an atmosphere of argon scrubbed by bubbling through a solution of chromous(II) and subsequently through a Zn/Hg amalgam in water. Milli-Q water was used in preparative reactions and purifications. $[Ru(NH_3)_5Cl]\bullet Cl_2$, 4-Chloropyridine, and trifluoroacetic acid were purchased from Aldrich. $NaPF_6$ was purchased from Strem. Tetrabutylammonium hexaflurophosphate ($[NBu_4]^+[PF_6]^-$) was purchased from Aldrich and dried under vacuum prior to use. The ^1H NMR spectra were obtained in deuterated solvents, D_2O or CD_3COCD_3, and recorded using a VXR 400 MHz FT-NMR.

1.2 Nano-patterning

Synthesis of β*-(dimethylamino)vinyl 2-pyridyl ketone*

3.9979 g of acetyl pyridine (0.033mol) and a slight excess of DMF dimethylacetal (4.7902 g, 0.0402) were dissolved in 30.0 mL of toluene. The reaction mixture was refluxed for 12 h with fractional distillation to remove MeOH generated by the reaction. The reaction was cooled to room temperature. Upon attempt to remove the solvent via rotovap, a yellow crystalline solid fell from solution. The solid was filtered from the solution and

washed with cyclohexane to yield 3.5502 g of β-(dimethylamino)vinyl 2-pyridyl ketone (54%). ^{1}H NMR data matched that reported in the literature.

Synthesis of the sodium salt of cytosine

To a solution of 0.325M NaOH in 95% ethanol, 2.0013 g of cytosine was added and stirred to maximum dissolution. The solution was filtered to remove any un-dissolved solid. The solution was then placed on the rotovap to remove solvent, leaving a white solid. Ethanol (abs.) was added to the solid and stirred overnight as a suspension. The suspension was filtered and the solid dried overnight under vacuum to yield 1.3657 g of the salt (77%).

1.3 Mononuclear Synthesis:

Synthesis of [Ru(NH$_3$)$_5$(pyCH$_2$SCH$_2$CH$_2$CN)]•2PF$_6$

200 mg of [Ru(NH$_3$)$_5$Cl]•Cl$_2$ was purged with argon and dissolved in 5.0 mL of water at 80°C. This solution was then added via syringe to 1.0 g freshly prepared Zn/Hg amalgam with 2 drops of trifluoroacetic acid (TFA) in 5.0 mL of water. This mixture was stirred at room temperature for 40 min. with bubbling argon. The reduced greenish yellow solution was then added via syringe to a solution of 3-(pyridin-4-ylmethylthio)propanenitrile (143 mg, 0.87 mmol) in 5.0 mL of water under argon and stirred for 2 h at room temperature. The resulting golden yellow solution was added to a 5.0 mL saturated solution of NaPF$_6$, stirred for 30 min. under argon and stored overnight at 4°C. The solution was filtered and the solid product washed with water and ether, then dried under vacuum to yield 79.0 mg

(18%). The pale yellow product was recrystallized twice using an acetone ether mixture (1:20, *v:v*).

^{1}HNMR (400 MHz, CD_3COCD_3) : δ (ppm) 2.47 (s, 15H, NH_3), 2.95 (t, 2H, CH_2), 3.48 (t, 2H, CH_2), 7.48 (d, 2H, py, J = 4.0), 8.49 (d, 2H, py, J = 4.88).

1.3 Binuclear Sythesis:

Synthesis of [Ru(NH$_3$)$_4$SO$_2$Cl]•Cl

500 mg of $[Ru(NH_3)_5Cl]•Cl_2$ was purged with argon and dissolved in 10.0 mL of water at 80°C. The solution was then cooled to room temperature and $NaHSO_3$ (0.7134 g, 6.86 mmol) was added and the mixture stirred at 80°C with constant bubbling of SO_2 gas. After 2 h, a tan precipitate formed and the solution was slowly cooled to room temperature over 2 h. The reaction mixture was then stirred at 0°C for 3 h to maximize precipitation. The solution was filtered and the solid was dried overnight under vacuum to yield $[Ru(NH_3)_4(HSO_3)_2]$, 345.8 mg (61%).

313.7 mg of $[Ru(NH_3)_4(HSO_3)_2]$ was dissolved in 20 mL of 6 M HCl and refluxed for 30 min. The salmon colored solution was then cooled to 0°C and stirred for 4.5 h resulting in a reddish–orange precipitate. The solution was filtered and the solid was washed with acetone. The solid was dried overnight to yield 116.0 mg of $[Ru(NH_3)_4SO_2Cl]•Cl$ (40%).

Synthesis of [Ru(NH$_3$)$_4$SO$_4$(4-Clpy)]•Cl

96.9 mg of $[Ru(NH_3)_4SO_2Cl]•Cl$ was dissolved in 7 mL of 0.1 M $NaHCO_3$. This solution was then added to finely distributed 4-chloropyridine (40 mg, 0.35 mmol) and stirred under argon for 2h. 2.0 mL of 6 M HCl with 5.0 mL of H_2O_2 was added to the reaction mixture and stirred for 30 min. 100 mL of acetone was added and the reaction mixture

was stored at 4°C overnight. The resulting solid was filtered from solution, washed with acetone and air dried to yield 80.8 mg of $[Ru(NH_3)_4SO_4(4\text{-}Clpy)]\bullet Cl$ (61%)

$[(4\text{-}Clpy)Ru(NH_3)_4(pyz)Ru(NH_3)_4(4\text{-}Clpy)]\bullet 4PF_6$

80.8 mg of $[Ru(NH_3)_4SO_4(4\text{-}Clpy)]\bullet Cl$ was dissolved in 1.5 mL of water and degassed with argon for 20 min. The solution was then added via syringe to 500 mg of freshly prepared Zn/Hg amalgam with 2 drops of TFA, and stirred for 1 h under argon. The reduced solution was then transferred via syringe to a solution of pyrazine (pyz) (7.8 mg, 0.10 mmol) in acetone (0.4 mL) and allowed to stir overnight in the dark. The solution was filtered and the solid was air dried to afford 33.6 mg of a powdery purple solid, $[(4\text{-}Clpy)Ru(NH_3)_4(pyz)Ru(NH_3)_4(4\text{-}Clpy)]\bullet 4Cl$ (31%).

The solid obtained above was dissolved in 5.0 mL of water and $NaPF_6$ (500 mg) was added to the solution and stirred 30 min. The solution was filterd and the remaining reddish purple solid was washed with water and then dissolved by washing the filter paper with minimal acetone into a separate flask. Ether was then slowly layered on top of the solution (20:1, Et_2O : acetone) and stored at 4°C overnight. The solution was filtered and the solid washed with ether and air dried. The solid was recrystallized a second time with an acetone ether mixture. The solid was collected, washed with ether and dried under vacuum to yield 8.8 mg of $[(4\text{-}Clpy)Ru(NH_3)_4(pyz)Ru(NH_3)_4(4\text{-}Clpy)]\bullet 4PF_6$ (17%).

^1H NMR (400 MHz, CD_3COCD_3) : δ (ppm) 4.62 (s, 24H, NH_3), 7.48 (d, 2H, py), 8.31 (s, 4H, pyz), 8.38 (d, 2H, py).

1.4 Electrochemistry

All cyclic voltammetry (CV) and differential pulse voltammetry (DPV) measurements were conducted using a Princeton Applied Research potentiostat 263-A. Solutions used in analysis were kept under an atmosphere of argon throughout the experiments. A three-electrode configuration was used consisting of a 1.5 mm glassy-carbon working electrode, a platinum wire counter electrode, and a saturated calomel electrode (KCl), separated from the solution by a glass frit, as the reference electrode. Prior to use, the working electrode was polished with an alumina slurry. The electrode was rinsed Milli–Q water, sonicated in Milli–Q, rinsed again with Milli-Q and finally with acetone after each polishing before experiments.

Oxidative electrochemistry was investigated in acetonitrile or pyridine using 0.10 M ($[NBu_4]^+[PF_6]^-$) as the supporting electrolyte, or in Milli-Q water brought to pH of 3 by addition of HCl. The analyte concentration was 1.0 mM. The electrochemical potentials were collected using Power Suite from Princeton Applied Research, and all data were collected at ambient temperature.

2 Results/Discussion

2.1 Electrochemistry of [Ru(py)4(thione)2]•2PF$_6$

The electrochemistry of the bisthione was conducted in pyridine due to degradation issues associated with exposure to various solvents. With a scan rate of 200 mV/s CVs were collected when the sample was initially preparation, 24 hours after sample preparation, and 96 hours after sample preparation (Figure 6). The CV clearly shows two waves one at E′ = 150 mV and the second at E′ = 213 mV.

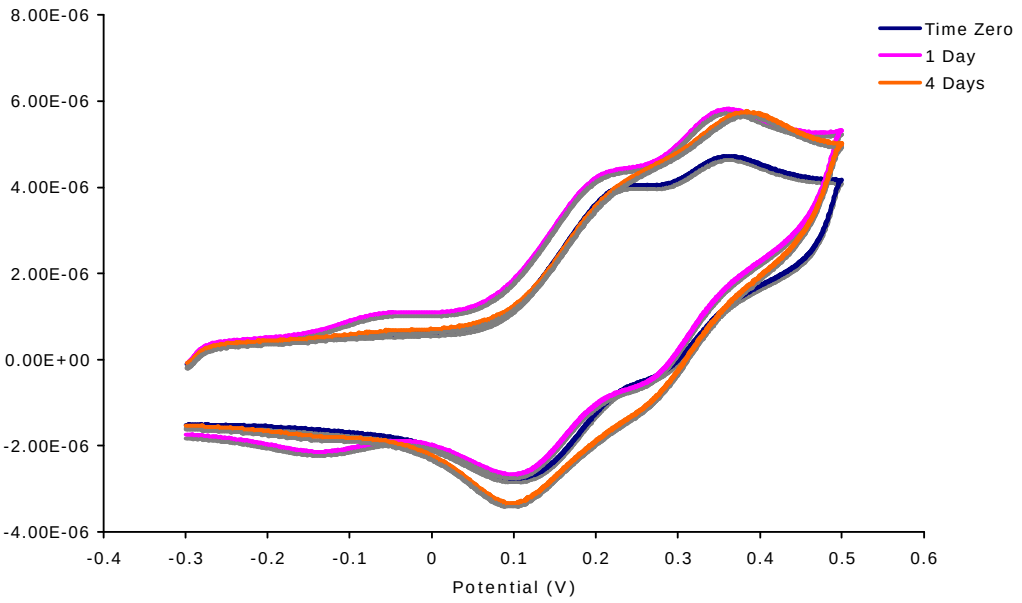

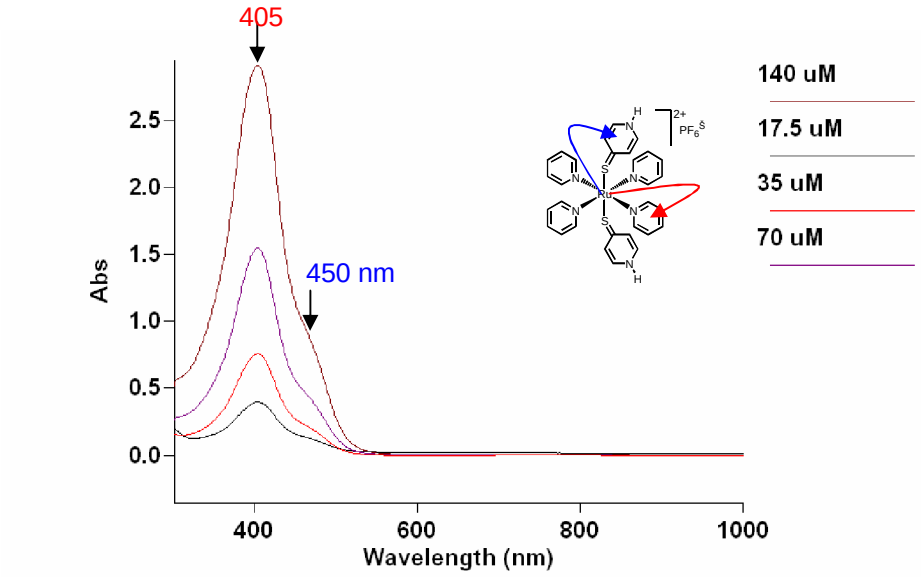

Figure 6

.

Variable time cyclic voltammogram of bisthione measured at 200 mV/s in a 1.0 mM solution of the analyte in pyridine with NBu_4PF_6 (0.1 M) as the supporting electrolyte.

UV-Vis experiments were also conducted on the bisthione at variable concentrations (Figure 7). Two electronic transitions were observed, one at 405 nm and the other at 450 nm, corresponding to ruthenium(II) to pyridine π* and ruthenium(II) to thione π* transitions respectively.[23]

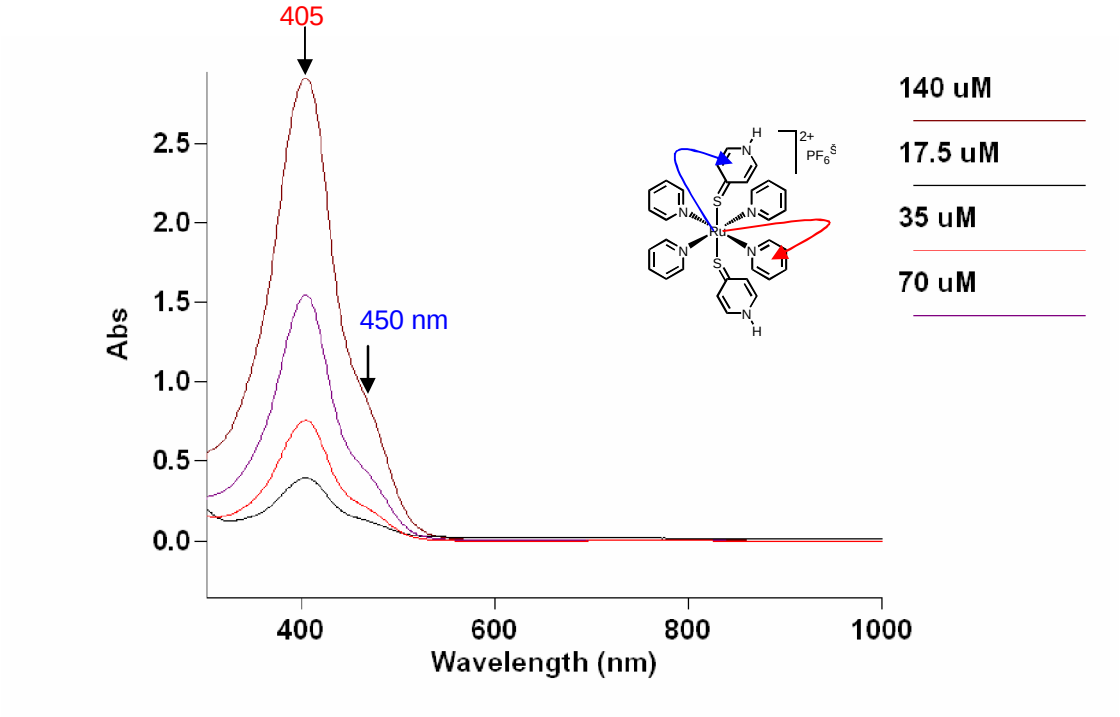

Figure 7: UV–Vis spectra of bisthione

2.2 Synthesis of Molecular Wires

The procedure outlined above for the preparation of dinuclear molecular wires has to date yielded mixed results. The binuclear compounds isolated in this procedure show extraordinary purity in the ^{1}H NMR, approximately 98-100%, however, oxidative electrochemical analysis of these complexes shows a three-wave pattern. If the sample were in fact pure, only two waves would be produced, one wave corresponding to each ruthenium center present in the molecule. The presence of a third wave at a potential

negative to that of the other two signifies the presence of impurities, the identities of which are not yet fully known.

Attempts to rectify this purity issue have been attempted by using Milli–Q water for all procedures, as well as scrubbing of the argon atmosphere. It is assumed that the main source of impurities is not in the procedure itself, but within tiny amounts of oxygen present during the binucleation reaction. The addition of the argon scrubber has shown a marked improvement in the purity of products; however, the temporary apparatus has flaws that at times may allow for oxygen to reenter the inert atmosphere. Due to pressure build-ups within the system, the rubber plugs that seal the various compartments have a tendency to pop off thus compromising the atmosphere. It is because of this, a new system of scrubbing chambers has been designed utilizing only glass and sealed metal connections (Figure 8) which will all but eliminate the possibility of compromising the atmosphere within this system. More care must also be taken in assuring the validity of the connections to reaction vessels.

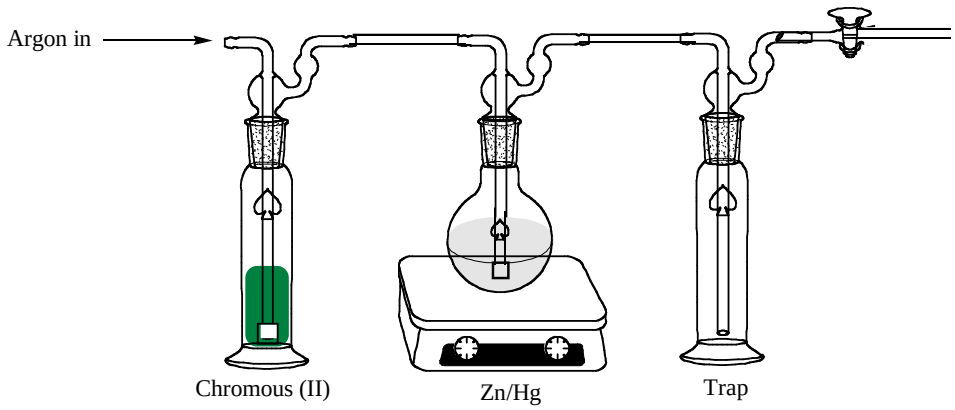

Figure 8: Proposed argon scrubbing system, steel springs to hold ground glass joints together not shown.

Conclusions

A viable route toward molecular wires has been established and binuclear precursors have been synthesized, however, purity issues are a major concern. A scheme has also been proposed for the formation of highly organized nano-patterned surfaces.

Future work will be directed toward the purity of both the mono- and binuclear ruthenium complexes. A synthetic route through the pentaammineruthenium aqua moiety and utilization of the dry box will be explored as it may offer a higher degree of purity in the formation of the mono-nuclear ruthenium complexes. If successful, we will attempt to use this moiety in the formation of the binuclear species as well.

Acknowledgements

I would like to thank my research advisor, Prof. Amar H. Flood, for his guidance. I would also like to thank Prem Chand for all of his insight into this project. I thank my lab mates for their support, and to the Indiana University Department of Chemistry for the use of all facilities.

References

1. Boncheva, M.; Whitesides, G. M. *MRS Bulletin* **2005**, *30*, 736.
2. Onclin, S.; Ravoo, B.; Reinhoudt, D. *Angew. Chem. Int. Ed.* **2004**, *44*, 6282.
3. Stöhr, M.; Wahl, M.; Galka, C. H.; Riehm, T.; Jung, T. A.; Gade, L. H. *Angew .Chem. Int. Ed.* **2005**, *44*, 7394.
4. Sessler, J. L.; Jayawickramarajah, J. *Chem. Commun.* **2005**, 1939.
5. Sessler, J. L.; Magda, D.; Furuta, H. J. *J. Org. Chem.* **1992**, *57*, 819.
6. Li, J.; Gold, B. J. *J. Org. Chem.* **2005**, *70*, 8764.
7. Auditore, A.; Tuccitto, N.; Marzanni, G.; Quici, S.; Puntoriero, F.; Campagna, S.; Licciardello, A. *Chem. Commun.* **2003**, 2494.
8. Auditore, A.; Tuccitto, N.; Quici, S.; Marzanni, G.; Puntoriero, F.; Campagna, S.; Licciardello, A. *Appl. Surf. Sci.* **2004**, *231*, 314.
9. Kang, J. F.; Ulman, A.; Liao, S.; Jordan, R.; Yang, G.; Liu, G. *Langmuir* **2001,** *17*, 95.
10. Classen, T.; Fratesi, G.; Constantini, G.; Fabris, S.; Stadler, F. L.; Kim, C.; de Gironcoli, S.; Baroni, S.; Kern, K. *Angew. Chem. Int. Ed.* **2005**, *44*, 6142.
11. Denmark, S. E.; Fan, Y. *J. Am. Chem. Soc.* **2002**, *124*, 4233.
12. Livoreil, A.; Dietrich-Buchecker, C. O.; Sauvage, J. *J. Am. Chem. Soc.* **1994**, *116*, 9399.
13. Jameson, D. L.; Guise, L. E. *Tetrahedron Lett.* **1991**, *32*, 1999.
14. Palacio, F.; Miller, J. S. *Nature* **2000**, *408*, 421-422.
15. Heath, J. R.; Ratner, M. A. *Physics Today* **May 2003**, 43-49.
16. Aviram, A.; Ratner, M. A. *Chem. Phys. Lett.* **1974**, *29*, 277.
17. Collier, C. P. e. a. *Science* **2000**, *289*, 1172.
18. Heinrich, A. J.; Lutz, C. P.; Gupta, J. A.; Eigler, D. M. *Science* **2002**, *298*, 1381.
19. Park, J. *Nature* **2002**, *417*, 722.
20. Liang, W. *Nature* **2002**, *417*, 725.
21. Coe, B. J.; Curati, N. R. M. *Comments on Inorganic Chemistry* **2004**, *25*, 147-184.
22. Joachim, C.; Gemzewski, J. K.; Aviram, A. *Nature* **2000**, *408*, 541-548.
23. Coe, B. J.; Meyer, T. J.; White, P. S. *Inorg. Chem.* **1995**, *34*, 593.